NON-STATIONARY ANALYSIS OF BAM 2003 EARTHQUAKE RECORD

Raimar J. Scherer [1], Amin Zahedi Khameneh [2] and Jörg Bretschneider [3]

[1] *Professor, Institute of Construction Informatics, Technische Universität Dresden, Germany*

[2] *Institute of Construction Informatics, Technische Universität Dresden*

[3] *PhD, formerly Institute of Construction Informatics*

Raimar.Scherer@cib.bau.tu-dresden.de, joerg.bretschneider@germanynet.de

ABSTRACT :

Strong ground motion is widely investigated by methods designed for stationary processes, as are power and Fourier or response spectra. In fact, it is a highly non-stationary phenomenon, whose characteristics are strongly linked to a theoretically well understood, but practically poorly apprehensible physical background. The catastrophic 2003 Bam, Iran, Earthquake has been analysed by others from seismological and engineering aspects, but frequency related parameters as well as non-stationary characteristics of this event have not been investigated so far. In this paper, we will investigate non-stationary properties of local strong motion by means of Evolutionary Power Spectra as well as by Time-dependent Principal Correlation Axes (TPCA) – a family of methods for local strong motion analysis developed by Bretschneider & Scherer (2000a 2000b, 2004, 2006), similar to well-known Principal Component Analysis. We use these methods to identify major wave phases and estimate the directions of motion as well as other specific characteristics of the corresponding wave trains. The findings for the strong motion record at Bam are then discussed with respect to source dynamics. Our findings on the faulting process are in very good agreement to those from aftershock analysis by Nakamura et al. (2005).

KEYWORDS: Bam Earthquake, Seismic Waves, Evolutionary Spectrum, Principal Correlation Axes, TPCA

1 INTRODUCTION

Seismic strong ground motion is a three dimensional, highly complex process. Because of the heterogeneity of the structure and the uncertainty of material properties of the earth's upper crust, strong ground motion is frequently modelled as stochastic process, and stochastic quantities are examined in order to predict the possible load on structures and buildings. The main non-stationary characteristic of earthquake acceleration records, from the structural engineering point of view, is the presence of transient wave trains with different kinds of particle movement, different spectral characteristics, amplitude and duration.

Non-stationary analysis can reveal both dominant frequencies and certain temporal patterns in the seismic records, which are related to specific characteristics of the wave trains comprising the overall strong motion at the site and to general mechanics of an earthquake source. The patterns in turn allow us to identify the wave types of each wave train and to estimate seismological as well as engineering parameters. While non-stationary analysis has been focused onto mid-range strong motion records and has been used mostly to asses empirically parameters for seismic load models so far, it can also be applied to investigate strong motion records from the epicentral area of an earthquake in order to reconstruct the rupture process.

In this paper, after a short review of seismological and engineering information on the Bam Earthquake, as well as a short overview over the non-stationary analysis methods applied, we will present and discuss evolutionary spectra as well as a full 3D TPCA analysis of wave patterns in a record directly upon the fault of the main shock of that earthquake. Results are then compared to those obtained by Nakamura et al (2005) via aftershock analysis.

2 THE BAM 2003 EARTHQUAKE

2.1 Tectonic setting and rupture

The Mw 6.6 Bam earthquake occurred at 01:56:52 UTC on December 26, 2003 close to the town of Bam near Kerman in South-eastern Iran. At least 26.371 people have been killed, 30.000 have been injured, and 70% of buildings have been destroyed in the Bam area during the main-shock, as estimated by local government.

The tectonics of the Bam region is dominated by the convergence between the Arabian and Eurasian plates, trending N to NNE at velocity ranges from 25-35mm/yr as deduced from GPS measurements (e.*g., McClusky et al., 2003*) and according to the NUVEL-1 model *(DeMets et al., 1990)*. To the west, the northwest-trending Zagros fold and thrust belt, which is an active continental collision zone, accommodates about 10mm/yr of NNE-trending shortening (Talebian and Jackson, 2002); in several areas further north, the crust is also forced to accommodate the convergence by shortening.

The most obvious fault in the area is the escarpment running for ~12 km south from the Posht river, between Bam and Baravat. It is clearly visible in satellite imagery (Fig. 1a) and in the field, and is mentioned in several earlier publications on the area (e.g. Walker & Jackson 2002). Source mechanism solutions (Eshghi & Zaré, 2003; USGS, 2003) show that the earthquake was induced by strike-slip faulting 7km south of Bam, at around 7km depth. All studies agree that the bulk (>80%) of the moment was released by almost vertical, nearly pure strike-slip faulting beneath the surface ruptures observed south of Bam, with the main slip occurring over a distance of about 12 km running from the southern limit of the surface ruptures. In the supplementary on-line material of their initial report, Talebian et al. (2004) pointed out that the long-period P and SH waveforms of the main shock could not be explained by a single centroid source with a strike-slip mechanism.

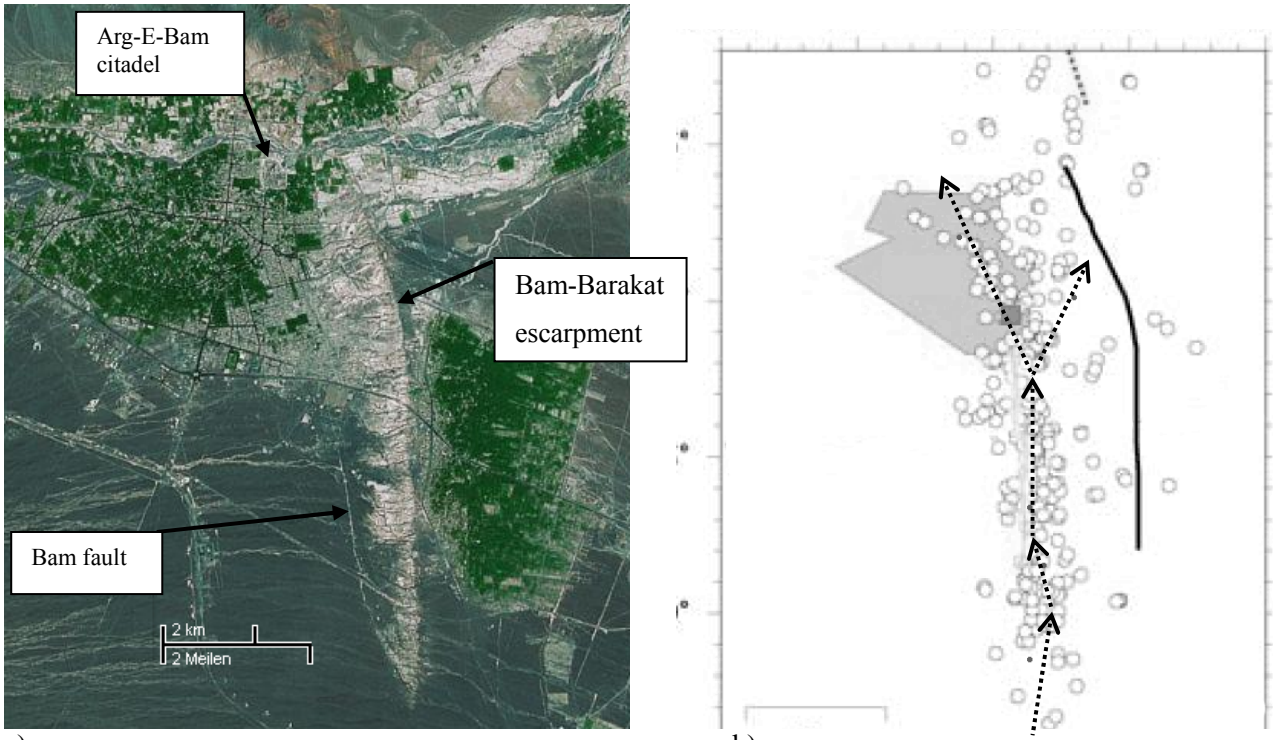

Fig. 1 a) Satellite image of the epicentral region of the 2003 Bam Earthquake (© Google Maps).

b) Aftershock locations (circles) and surface projection of the Arg-e-Bam fault proposed by Nakamura et al. (dotted arrows indicate rupture propagation) + edge of the Bam-Baravat escarpment (solid line). The small square indicates the location of the recording instrument in Bam.

2.2 Ground motion records

Ground motion produced by the Bam Earthquake was recorded in the centre of Bam city by a digital accelerometer operated by the Building and Housing Research Centre of Iran (http://www.bhrc.gov.ir/) (Fig. 2). PGA of 0.98g and 0.887g were recorded in the vertical and horizontal components at the site, which has been categorized by Zaré & Hamzehloo (2005) in UBC soil class 3 (average shear wave velocity in the first 30 meters 300 to 500 m/sec) due to the site fundamental frequency, which was found to be in the range of 2-5Hz.

The dominant feature of the ground motion is a high-amplitude, long period E–W pulse, transverse to the fault, with 1.2m/s peak velocity and 0.4m peak displacement. At around 3s, there is even stronger vertical motion, while the N–S motions are relatively small. These characteristics correspond to those theoretically expected near the fault for a N–S trending right-lateral strike-slip fault with rupture propagating northwards towards the site.

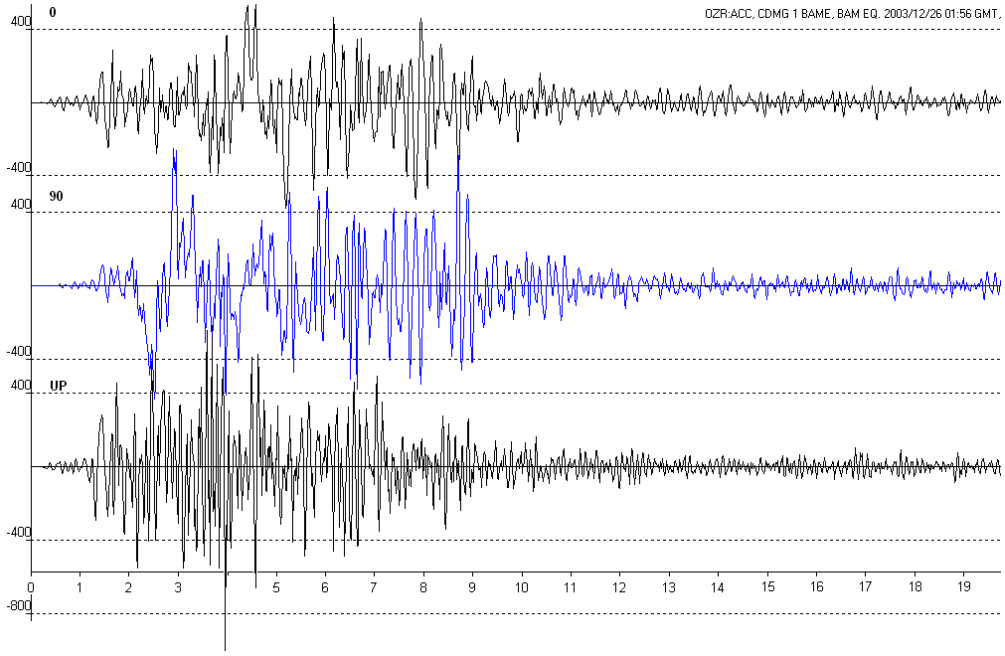

Fig. 2 Acceleration components of the BAM 2003 main shock recorded at Bam station, first 20 seconds

A seismic network consisting of 9 temporary stations had been installed to monitor aftershock activities in and around Bam from February 6 until March 7, 2004. Each station was equipped with a high sensitivity, velocity type, three-component seismometer with a natural frequency of 1Hz. A three-component strong motion accelerometer was also installed at the famous Arg-e-Bam citadel. The overall trend of the aftershock epicentre distribution is virtually linear along an approximately 20 km long axis in the N2ºW–S2ºE direction, parallel to a line about 3.5 km west of the geological Bam surface fault on the ground. Nakamura et al. (2005) propose a new ‘‘Arg-e-Bam fault’’ as the source fault to distinguish it from the Bam fault (Fig. 1b).

3 NON-STATIONARY ANALYSIS OF STRONG GROUND MOTION DATA

For reliable stochastic models of strong ground motion, the non-stationary characteristics of the seismic process, which originate from its constitution of several wave trains with specific, different characteristics as well as from the transient nature of each wave train, cannot be ignored. Because of its specific time and spectral characteristics, in a stochastic/statistic setting, each wave train must be treated per se as a different population. However, these wave trains stem from the same source, directly as for P and S waves, or indirectly as for reflected/refracted waves and surface waves, which suggests that there may be a common generic model.

Based on these principles, Scherer (1993) has proposed a general non-stationary load modelling approach, consisting of a division of the ground motion process into sub-processes associated with major, load dominant wave trains, and based on the evolutionary spectrum both for the seismic load model itself and for the separation of

the sub-processes. Bretschneider & Scherer (2000, 2002, 2004) have later suggested time-dependent principal correlation axes (TPCA) as the tool of choice to identify and distinguish the wave trains, and also a preliminary parametric load model for the transient sub-processes, based on the evolutionary spectrum of the first TPCA component. Bretschneider (2006) has further refined and extended this load model.

3.1 Evolutionary power spectral analysis

A common non-stationary load model which incorporates both spectral characteristics and time dependence is the evolutionary power spectrum (EPS), theoretically introduced by Priestley in 1965. In essence, the evolutionary spectrum describes energy (variance) distribution over the frequency and time domain of an ensemble of stochastic processes. Kameda & Sugito as well as Scherer, Riera & Schueller have proposed estimators for the evolutionary spectrum.

Generally, evolutionary spectral analysis of strong motion accelerograms seems to be a difficult task, as these spectra usually do not have a smooth surface. However, important information about wave trains and their spectral characteristics can be derived from normalized power spectra of the Bam record (Fig. 3)

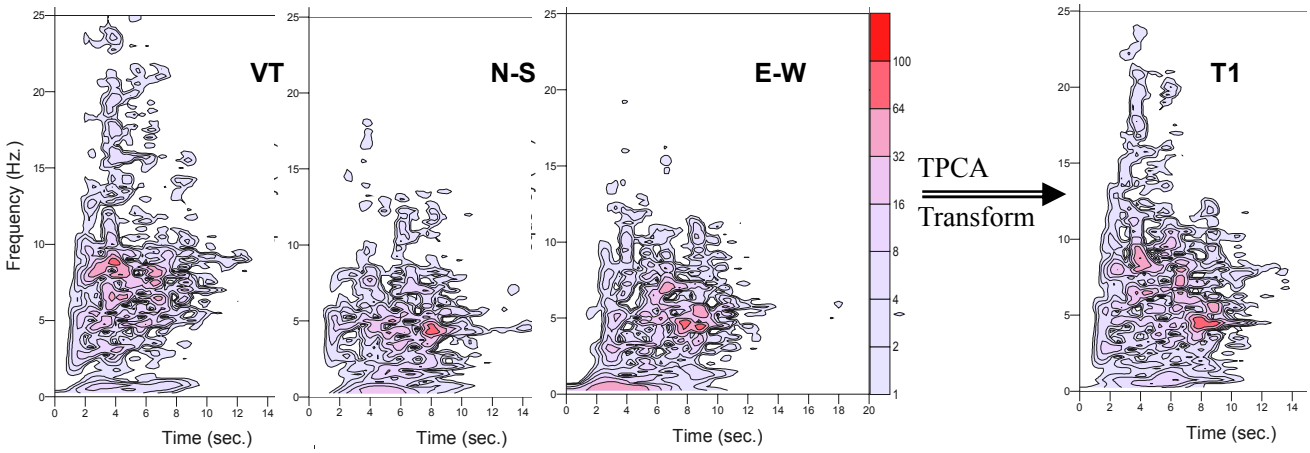

Fig. 3 Normalized logarithmic contour plots of the evolutionary power spectra of the Vertical, North-South & East-West components and of the main principal axis component T1 (right) of Bam record from Fig. 2.

In the EPS of the vertical component, onset of P-waves can be observed at around 1.2sec in a broad frequency range. Furthermore, at least two pronounced peaks can be identified at 3.8 & 6.6sec, most significant at frequencies of 9 Hz and 8.4 Hz, resp.. These peaks correspond to waves with vertical axis of motion; they may be interpreted as corresponding to new P-waves from a 2nd & 3rd rupture or from strong reflectors in the ground.

In the EPS of the horizontal components, onset of the first S-wave can be observed at the long enduring peak beginning at 1.6 sec at a very low frequency of about 0.5Hz, which clearly corresponds to the strong E-W pulse obvious in the accelerogram. A second strong peak occurs at (6.3s, 7Hz) in the E-W, but the strongest peak at 8sec with a dominant frequency of 4.5Hz in both components. These peaks correspond to waves with predominant horizontal motion, i.e. S waves or Love surface waves. Again, it is possible to interpret this as indicating a second and third rupture segment producing S-waves of higher frequencies.

The right side of Fig. 3 presents the EPS of the first time-dependent principal component T1 determined by the TPCA method with a constant window length of 1.5sec and 20% window overlap, which resides on a time-variable principal axis aligned with the course of the dominant direction of acceleration. The peaks of all original components are clearly conserved, even pronounced. T1 has therefore been proposed by Bretschneider & Scherer (2000, 2004, 2006) as a reference component for seismic hazard analysis and load prediction.

3.2 Time-Dependent Principal Correlation Axes Analysis

Principal Correlation Axes were originally suggested by Penzien & Watabe (1975) for predictive load models as axes, where cross-correlation between the components of the 2D or 3D stationary stochastic process vanishes

and hence these components could be treated independently in a statistical sense. A 3D stochastic process upon those axes is completely described by three (auto-) covariances instead of six covariances of the symmetric Tensor in the general case. The idea has been picked up by Kubo & Penzien (1979) who described the properties of strong motion upon those axes. Bond (1980) was the first to apply TPCA to estimate those axes. His method has been improved by Scherer & Bretschneider (2000, 2004) and used for a comprehensive analysis of the 1994 Northridge Earthquake. Bretschneider (2006) has recently significantly improved and extended the estimator to all three principal axes, now called Spectrally Adaptive Principal Correlation Axes (SAPCA).

3.2.1 Principle of the TPCA approach

In short, the TPCA method can be described as an orthogonal, i.e. energy conserving, transformation $\mu^* = \mathbf{T}^T \mu \mathbf{T}$ of the coordinate system μ (e.g., $\mu = (0°,90°,VT)$ axes) of the recorded data in a way which enables to inspect more clearly the dominant and sub-dominant oscillations of the strong motion. This means, the data itself, which can only be recorded as overlaid projections of the spatial oscillations upon unavoidably fixed axes of the recording device, remain unchanged, just the view onto the data is changed. It turns out that for a n-D stochastic stationary process, the transformation matrix **T** which fits best to this goal consists of the Eigenvectors (T_1,T_2,T_3) of the correlation matrix μ of its components. As strong ground motion is a process which is not stationary as a whole, all quantities in question are time-dependent with respect to limited stationary time intervals.

After the transformation $\mathbf{A}^* = \mathbf{T}^T \mathbf{A}$ of the data $\mathbf{A} = (a_0;a_{90};a_{VT})$, cross-correlation of the new acceleration components $\mathbf{A}^* = (T1;T2;T3)$ becomes zero, and the Eigenvalues λ of the diagonal matrix μ^*, which are indeed the variances (= energy) of the components of $\mathbf{A}^*$, exhibit a clear distribution to a maximal, intermediate and minimal value. The component T1 corresponding to λ_{max} characterises the direction of the energetically dominant oscillation – in our case soil acceleration – in the time window where μ has been estimated. While TPCA works with fixed windows, the SAPCA method first applies a local spectral estimate to determine appropriate window length, which is crucial for optimal resolution without loosing statistical significance.

As elaborated in Scherer & Bretschneider (2000), the course of the main principal axis T_1 reveals significant patterns, which can be analysed by T_1's strike angle θ and elevation angle φ, defined similar to strike and rake of the slip vector in source mechanics. In a moderate distance to the rupture, high elevation indicates P-waves or Rayleigh waves, while low elevation corresponds to S waves and Love waves. Steep ascent or descent of elevation indicates a change of dominance from P to S waves and vice versa. The peaks of principal variance σ_1 within those P/S dominance intervals are useful to assess the intensity as well as the actual extension of the respective wave trains. Indeed, the principal variances are identical to the RMS functions of the principal axis components. θ is an indicator of the direction of transverse motion, most significant if elevation φ is low.

4 TPCA ANALYSIS OF BAM RECORD

For the data of the Bam earthquake shown in Fig. 2, strike and elevation of time-dependent principal correlation axes as well as principal variances have been estimated by the TPCA method for various window lengths. To investigate local non-stationary features in detail, we demonstrate them for a window length of 0.5s in Fig. 4. For proper interpretation of these graphs, one should understand that principal axes always form an orthogonal tripod; that each principal axis is associated with different wave trains over the course of the record or vice versa, that every wave train in the record is mapped onto different principal axes in a well defined manner, caused by its transient character and its relative rank in terms of energy. This is best observed at the principal variances σ. It is essential to investigate angles and variances together and to take into account the cumulative effect of overlaid waves with resembling directions of motion, as well as geometrical attenuation and directivity effects.

In Fig. 4, it can be seen from the σ diagram that the thick, thin and dotted curves refer to the principal axis with maximum, medium and minimum variance (energy). Elevation φ_1 has three "hills", starting at 0s, until 7.2s, indicating dominance of P waves, and quite low φ_1 phases from 2.7-2.9s, 4.9-6.3s and 7.2-11s, indicating dominance of waves with mostly transverse motion. The steep descents/ascents of φ_1 (and φ_2) mark the transition of dominance. Principal variance σ_1 has several pronounced peaks, each of which belongs to a transient wave train.

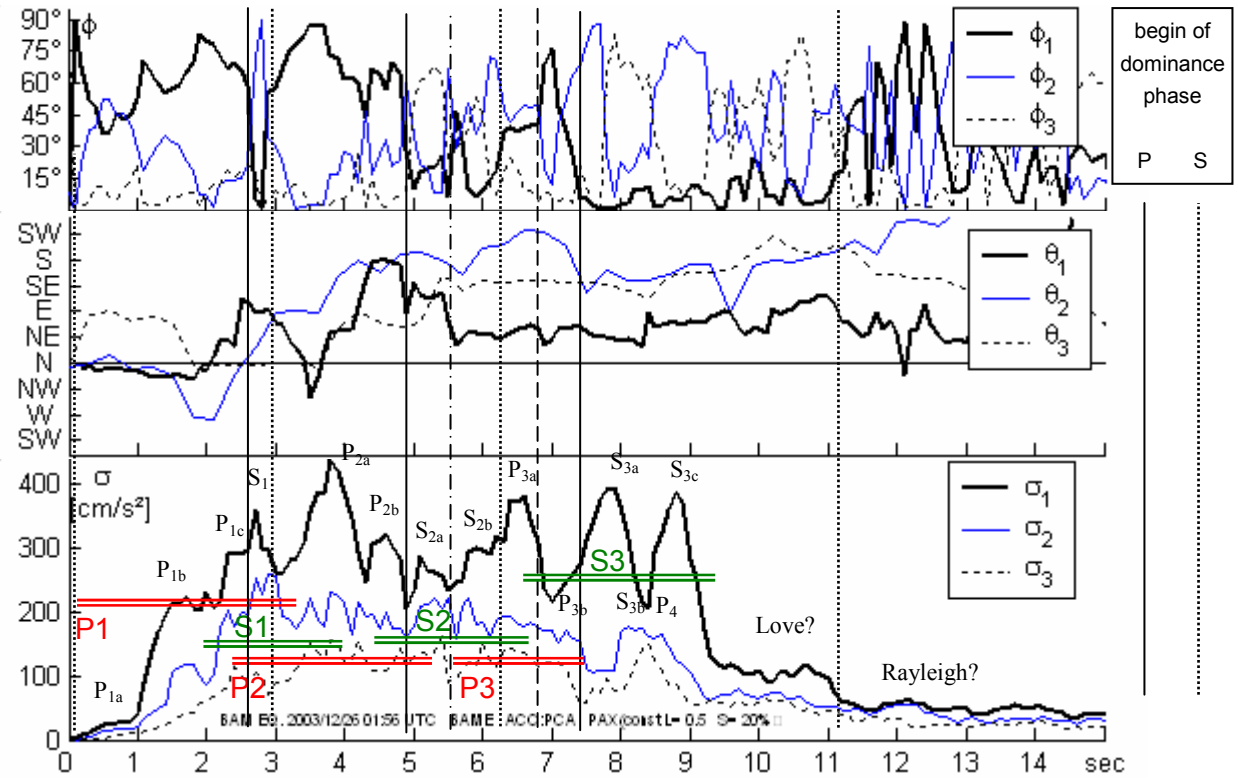

Fig. 4 Elevation and strike angles φ and θ of the principal axes T_i and corresp. principal variances $\sigma_i = \sqrt{\lambda_i}$ for the Bam record in Fig. 2, estimated by the TPCA method with a window length of 0.5s.

The first peaks $P_{1,abc}$ clearly belong to direct P waves, as elevation φ_1 is high. Peak S_1 at 2.6s belongs to direct S waves (see the SH pulse in Fig. 2), its slope starts in σ_2 at about 2s, subdominant to earlier P waves, and is set forth in σ_2 at 3s. Likewise, the ascending and descending slopes of σ_1-peak P_{2a} at 3.7s are clearly visible in σ_2 from 2.5-3s and 4.2-4.8s, as well as those of peak P_{2b}, again P waves. What follows are again two strongly dominant shear wave trains (φ_1 low) with σ_1-peaks S_{3a} and S_{3c} at 7.8 and 8.8s. Note that the slope of S_{3a} is in σ_3 and that there are subdominant S and P waves whose peaks S_{3b} and P_4 which have slopes both in σ_2 and σ_3.

These three pairs of P-S phases, outlined in Fig. 4 as P1/S1, P2/S2, P3/S3, do not belong to a single-phase source, but can be interpreted as stemming from three separate rupture phases. Inspecting strike angles θ (displayed in cardinal points) shall now reveal the orientation of the rupture segments.

For S1, θ_1 = E(ast) at 2.7s is continued subdominantly by θ_2 until 3.5s. For the ascending slope of S_1 at 2s, θ_2 = W is equivalent to E. As θ for S waves indicates the transverse axis of particle motion, we conclude that orientation of the first rupture segment is N-S. Additionally in this case, the P wave fellow of S_1, P_{1b}, has an inclined incidence (=principal) axis ($\varphi_{1/2} \approx 60°/30°$). Hence θ_1/θ_2 can be trusted and indicate the direction of P wave propagation. Both θ_1/θ_2 point almost N(orth), which supports our conclusion for the first rupture segment.

However, it is not safe to interpret θ_1 for P2, between 3 and 4.9s, as the principal axis T_1 of the P2 P waves is almost vertical, hence its minor projection into the horizontal plane maybe subject to noise and secondary effects. Nevertheless we can trust θ in the second phase S2 of shear waves, and find that at the dominance transition point between its two peaks S_{2a} and S_{2b}, marked by a dash-dot line, θ_1 switches from SE to almost NE. Taking into account that both P2 and S2 have two peaks in similar relation to each other, we conclude that the second rupture phase has two segments and that the rupture divided into two branches, one propagating NW (transverse to SE), towards the site, and another running NE, away from the site, hence its P and S waves arrive 1s later.

In the third phase of dominant P waves, from 6.2 to 7.3s, there is an interesting transition, apparently between two different P waves. Both φ_1,φ_2 initially show intermediate elevation, i.e. inclined incidence, and at 6.8s (dotted line), there is an immediate uprise of φ_1 to 90°, accompanied by a shift in strike θ_1. Typical for a dominance

transition was a changing intensity trend (a notch in σ), but σ_1 reveals that these shifts of the principal axis T_1 clearly occur in the midst of the slope of the σ_1-peak P_{3a}, i.e. within one and the same wave train.

Our interpretation of this is that a non-vertical (45°) strike-slip rupture has been passing by the site in very close distance, rising up the principal axis by P waves directly from beneath the site at the moment of crossing, which are immediately subdued by fellow S waves, but we can see them in T_2 (P_{3b}, high elevation φ_2).

An explanation for the intensity of the S waves in the third phase, which are as strong as those of S1, is that the generating rupture is now much closer to the site than the initial, more distant rupture phase; hence the waves are only slightly attenuated. There are two distinguished peaks, whose strike θ_1 is stable NE with a sharp shift of 25° towards ENE at the transition point, which may again point to an asperity on the fault which caused the rupture to deviate. As θ shows the transverse of propagation, the third rupture segment points from SE to NE.

Note that there is another vertical motion (peak P_{3b}) in σ_2 which remains subdominant and whose corresponding high elevation ($\varphi_3|\varphi_2$ before/after the transition) continues as a plateau in $\varphi_2|\varphi_3$ and, from 11s, even in φ_1. It could be that these long enduring, combined horizontal and vertical motions are Rayleigh and/or Love waves generated e.g. by the surfacing rupture or at the Bam fault system.

Our findings are in excellent agreement with results obtained by Nakamura (2005) from aftershock distributions. Fig. 5 shows the strike angles σ_1 plotted into a map of the rupture zone, presentation is divided into four intervals for better readability. The solid line is the fault line identified by Nakamura, strike is drawn dashed at Bam site.

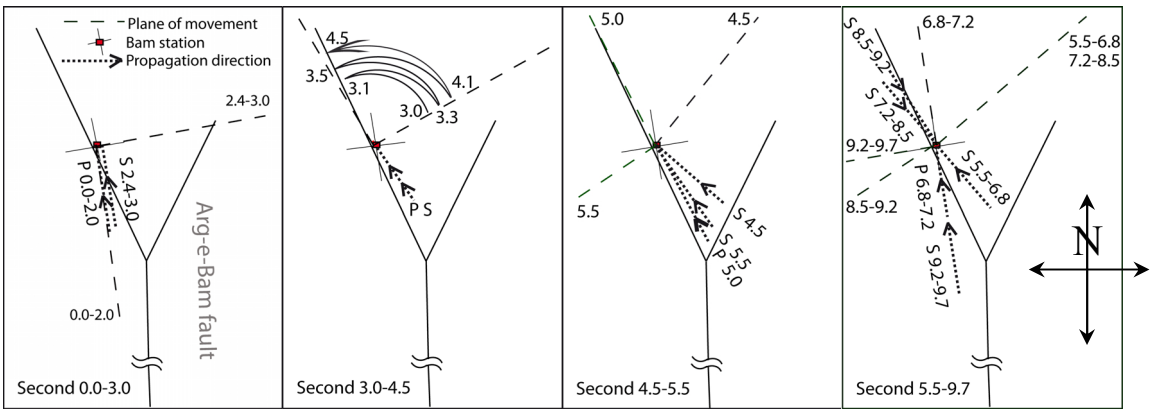

Fig. 5 Development of the strike angle θ in time intervals (dash lines, values in sec).

5 CONCLUSIONS

The non-stationary features of the Bam record from the rupture zone of the Bam (2003) Earthquake have been analysed by evolutionary spectra and time-dependent principal correlation axes. It turns out that the assembly of wave trains at the local site can be correctly decoupled and both the transient wave trains and significant parameters can be derived from patterns in the course of the time-dependent principal axes as well as the principal variances obtained by the TPCA method. Corresponding fundamental frequencies can be obtained from the evolutionary spectrum. While elevation angle of the principal axes is useful to distinguish the wave type, the strike angle θ carries information on the orientation of the shear wave trains and, in some cases, also of waves with vertical motion. Additionally, the variance of the principal axes reveals the proportional energy and duration of the wave trains. The principal axes exhibit associated temporal patterns, which can be used to analyse the local wave field and, in records close to the rupture zone, to derive information about rupture segmentation and asperities on the fault.

Our conclusions from the non-stationary TPCA analysis of the Bam record for the rupture movement of the 2003 Bam, Iran Earthquake are in excellent agreement with results obtained from other methods accepted by seismologists, especially the fault lines obtained by Nakamura et al. (2005) from their analysis of aftershock distributions. Furthermore, a passing by fault, crossing under a recording station, was identified the first time.

Our analysis does not validate the suitability of the TPCA method for analysis of rupture processes in general, as only one strong motion record was available. But given more records from the rupture zone, it should be possible to reconstruct reliably the major fault lines, which is one of the targets of further research on application of TPCA in strong ground motion analysis.

REFERENCES

Bond, W.E. (1980). A study of the engineering characteristics of the 1971 San Fernando Earthquake records using time-domain techniques, Ph.D. Thesis, Rensselaer Polytechnical Institute, New York

Bretschneider, J. & Scherer, R.J. (2000). Non-stationary Reference Seismograms. *XXVII General Assembly of the European Seismology Commission,* Lisbon 10-15th Sept. 2000, Proc. 409-413.

Bretschneider J. & Scherer R.J. (2004). Multi-wave, non-stationary, parametric load model for seismic hazard assessment and prediction. *13th World Conf. Earthqu. Eng.,* Vancouver, B.C. , Paper No. 2587

Bretschneider, J. (2006). Ein wellenbasiertes, stochastisches Modell zur Vorhersage der Erdbebenlast, Ph.D. thesis (Dissertation), Technical University of Dresden, Dep. Civil Eng., Germany, 2006, **http://nbn-resolving.de/urn:nbn:de:swb:14-1183717691264-79760**

Eshghi, S. & Zaré, M. (2003). Bam (SE Iran) earthquake of 26 December 2003, Mw 6.5:A preliminary reconnaissance report. http://www.iiees.ac.ir/English/bank/eng_databank.html .

Jackson, J., Bouchon, M. et al. (2006). Seismotectonic, rupture process, and earthquake-hazard aspects of the 2003 December 26 Bam, Iran, Earthquake. *Geophys. J. Int.* **166**, 1270–1292.

Kameda, H. & Sugito, M. (1984). Prediction of Strong Earthquake Motions on Rock Surface Using Evolutionary Process Models. *Proc. Int. Conf Struct. Analysis & Design of Nuclear Power Plants,* Porto Alegre, 161-186

Kubo T. & Penzien J. (1979). Analysis of Three-dimensional Strong Ground Motions along Principal Axes, San Fernando Earthquake. *Earthq. Eng. and Struct.Dynamics* **7**, 265-278

Nakamura, T. et al. (2005). Source fault structure of the 2003 Bam earthquake, southeastern Iran, inferred from the aftershock distribution and its relation to the heavily damaged area: Existence of the Arg-e-Bam fault proposed, *Geophys. Res. Lett.*, 32, L09308, doi:10.1029/2005GL022631.

Penzien J. & Watabe, M. (1975). Characteristics of Three-Dimensional Earthquake Ground Motion. *J. Earthq. Eng. And Struct. Design* **3**, 365-373.

Priestley, M. B. (1965). Evolutionary spectra and non-stationary stochastic processes. *J.Roy.Stat.Soc.* **27 No. 2**, 1965, pp 204–237

Sadeghi, H., Fatemi Aghda, S.M., Suzuki, S & Nakamura, T. (2006). 3-D velocity structure of the 2003 Bam earthquake area (SE Iran): Existence of a low-Poisson's ratio layer and its relation to heavy damage. *Tectonophysics* **417 No. 3-4**, pp 269–283.

Scherer, R.J. & Bretschneider, J. (2000), Stochastic Identification of Earthquake Wave Entities, 12th WCEE, Auckland, 2000, Book of Abstracts, Paper 2436

Talebian, M. & Jackson, J.A. (2002). Offset on the main recent fault of NW Iran and implications for the late Cenozoic tectonics of the Arabia–Eurasia collision zone. *Geophys. J. Int.* **150**, 422–439.

Talebian, M. et al. (2004). The 2003 Bam (Iran) earthquake: rupture of a blind strike-slip fault. *Geophys. Res. Lett.* **31**, L11611.

Walker, R., Jackson, J.A. (2002). Offset and evolution of the Gowk fault, S.E. Iran: a major intra-continental strike-slip system. *J.Struct. Geol.* **24**, 1677–1698.

Zaré, M. & Hamzehloo, H. (2005). Strong Ground-Motion Measurements during the 2003 Bam, Iran, Earthquake. *Earthquake Spectra* 21, S1, 165–179.